Identifying the Role of Primary and Secondary Interactions on the Mechanical Properties and Healing of Densely Branched Polyimides

Arijana Susa[a], Anton Mordvinkin[b], Kay Saalwächter[b], Sybrand van der Zwaag[a], Santiago J. Garcia*[a]

[a] Novel Aerospace Materials group, Faculty of Aerospace Engineering, Delft University of Technology, Kluyverweg 1, 2629 HS, Delft, The Netherlands
[b] Institut für Physik – NMR, Martin-Luther-Universität Halle-Wittenberg, Betty-Heimann-Strasse 7, 06120 Halle (Saale), Germany

*e-mail: s.j.garciaespallargas@tudelft.nl

List of figures and tables:

Rheology – temperature sweeps

The rheological temperature sweeps were performed in the cooling ramp, at 1 °C/min cooling rate and the results are shown in Figure S1 and were already discussed in our previous article.[1] The temperature range selected (0-50°C) is showing the transition from the glassy to the dissipative regime of the polymer relaxation (T_g), which plays an important role in the self-healing (SH) mechanism of these polymers, as previously reported.[2,3] The maximum of the *tan δ* peak is taken to be the optimal healing temperature (T_{SH}), since it represents the maximum viscous dominance ($G'' > G'$), i.e. maximum mobility for healing, and it is responsible for the first healing step.[2,3] Figure S1a shows the storage modulus (G') and loss modulus (G'') curves while damping factors (*tan δ*) versus temperature at 1 Hz for all the samples studied are shown in Figure S1b. The $T(tan\ \delta_{MAX})=T_g=T_{SH}$ values are given in Table I.

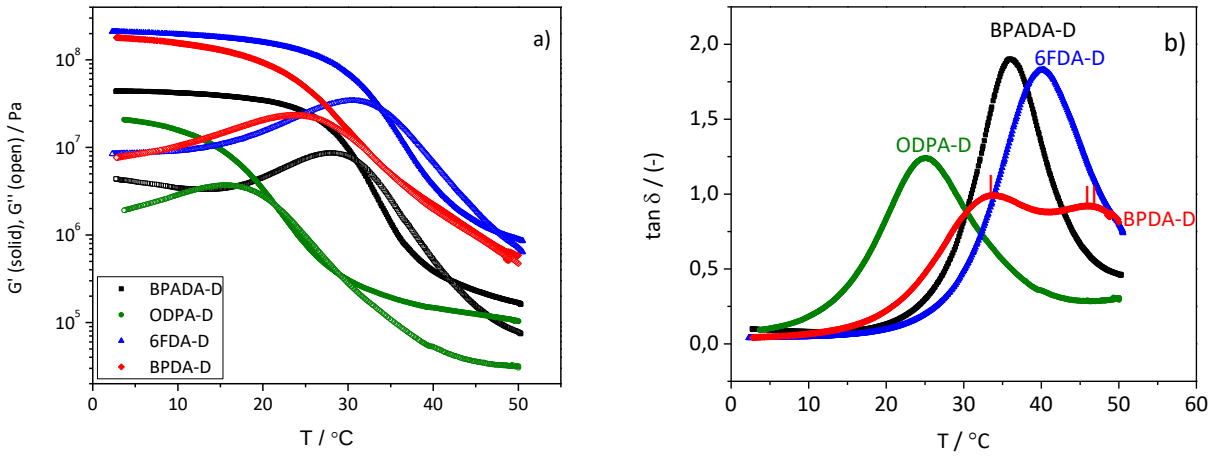

Figure S1. a) Storage (G') and loss (G'') moduli and b) *tan δ* curves from the rheological temperature sweeps experiments, showing distinct T_g-relaxations of the four PIs.

[1] Susa, A.; Bijleveld, J.; Hernandez Santana, M.; Garcia, S. J., Understanding the Effect of the Dianhydride Structure on the Properties of Semi-aromatic Polyimides Containing a Biobased Fatty Diamine. *ACS Sustainable Chemistry and Engineering* **2018,** *6* (1), 668–678. DOI: 10.1021/acssuschemeng.7b03026

[2] Susa, A.; Bose, R. K.; Grande, A. M.; van der Zwaag, S.; Garcia, S. J., Effect of the dianhydride/branched diamine ratio on the architecture and room temperature healing behavior of polyetherimides. *ACS Applied Materials & Interfaces* **2016**, 8 (49), 34068–34079.

[3] van der Kooij, H. M.; Susa, A.; García, S. J.; van der Zwaag, S.; Sprakel, J., Imaging the Molecular Motions of Autonomous Repair in a Self-Healing Polymer. *Advanced Materials* **2017**, 1701017-n/a.

Tensile test

Tensile parameters – undamaged samples (pristine)

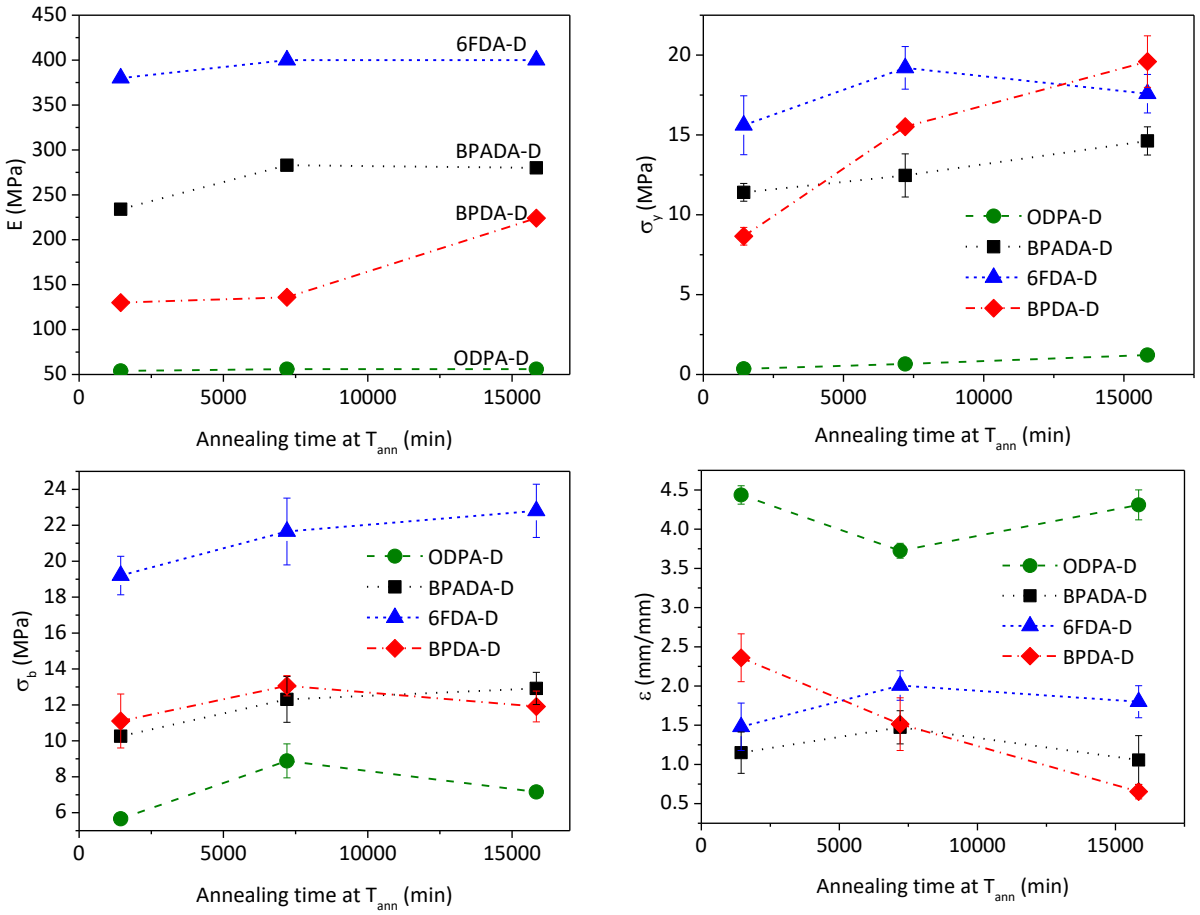

Figure S2. The effect of dianhydride structure and annealing time at T_{ann}=T_{SH} on the Young modulus (E), stress at yield (σ_y), stress at break (σ_b) and strain at break (ε_b) of the pristine materials.

Effect of testing temperature on the mechanical and healing properties

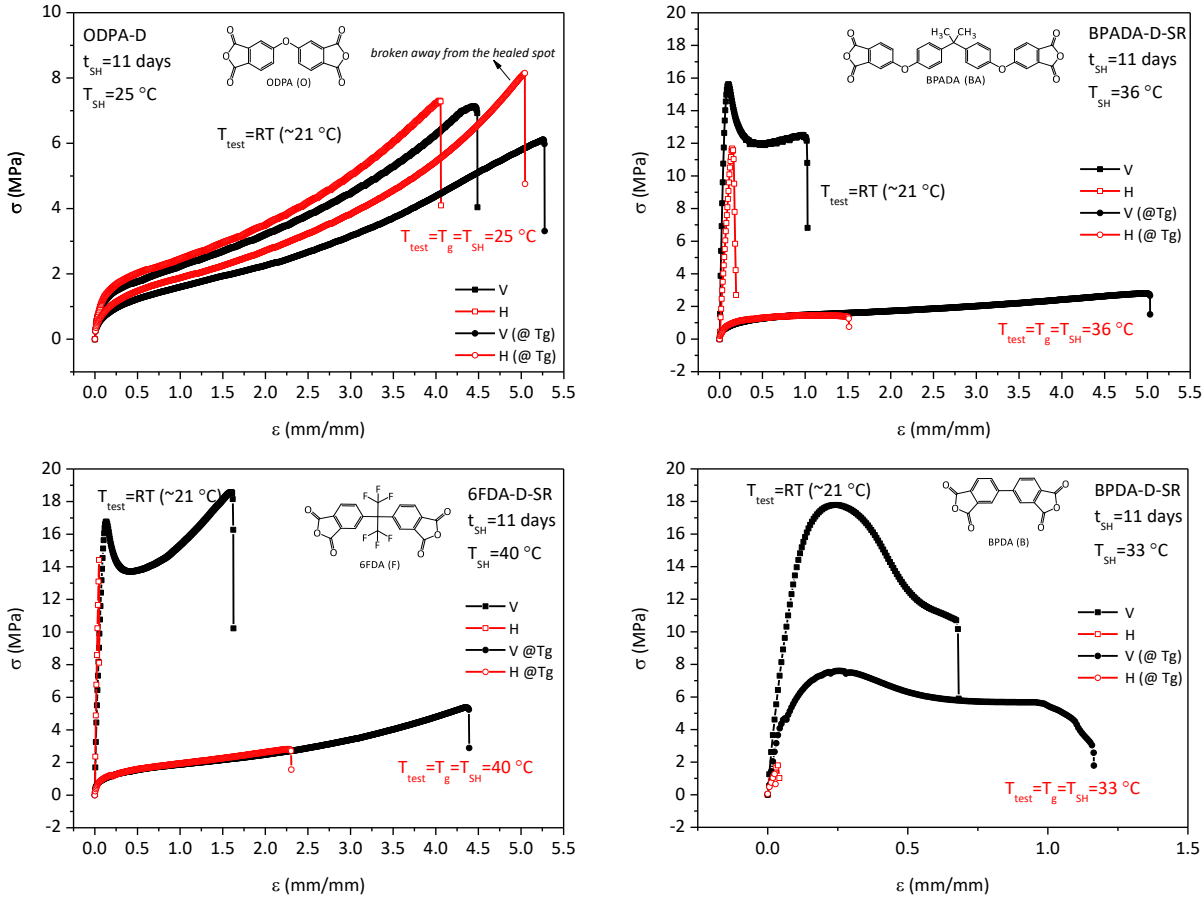

Figure S3. Stress-strain curves at 80 mm/min strain rate showing the effect of the testing temperature on the general mechanical performance of pristine (V) and samples healed at their T_{SH}=T_g for 11 days (H).

Rheological parameters

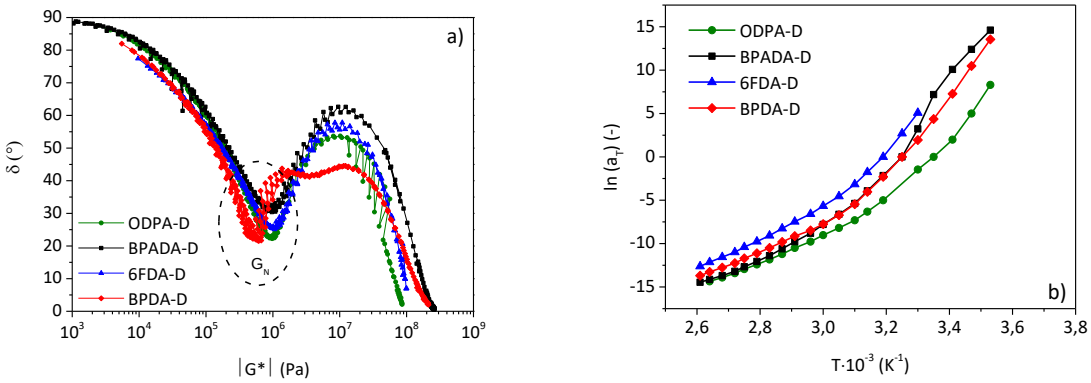

Figure S4. a) van Gurp-Palmen plot used for M_e calculations in Table II; b) horizontal shift factors (a_T) from the TTS mastercurves.

Synthesis of the Non-Aromatic PI (reference)

In order to evaluate the effect of the aromatic interactions on the rheological behavior of the PIs in this work, a non-aromatic PI (named **DCDA-D**) was prepared as a reference. Since DCDA dianhydride does not contain any linker between the cyclohexyl units, it can be considered a non-aromatic analogue of the BPDA dianhydride (See Scheme S1). An alicyclic dianhydride dicyclohexyl-3,4,3',4'-tetracarboxylic dianhydride (**DCDA**) (99%, Advanced Organic Synthesis LLC) was reacted with the previously used fatty dimer diamine (Priamine 1075™, here named **DD1**) (Croda Nederland B.V.). The amounts of each monomer were added at the theoretical stoichiometric ratio, calculated according to the molecular weights of the monomers (MW_{DCDA}=306.31 g/mol and MW_{DD1}=536.80 g/mol) and assuming both chemicals are 100% difunctional. The synthesis was conducted following the same procedure as for the other (aromatic) PIs in this work.[1, 2] The only difference was that the DCDA-based polymer remained soluble in the polymerization solvent (DMAc) even upon cooling down to room temperature, as opposed to the aromatic PIs. For this reason, the DCDA-D polymer did not precipitate from the solution. Vacuum distillation was performed at 70 °C and 10 mbar for one hour and after that the usual drying and annealing protocol was continued (as for the aromatic PIs) to yield the specimens. The polymer obtained appeared softer, tackier and much less colored (light yellow) than the aromatic ones (dark yellow to brown). The general properties are shown in Table S-I.

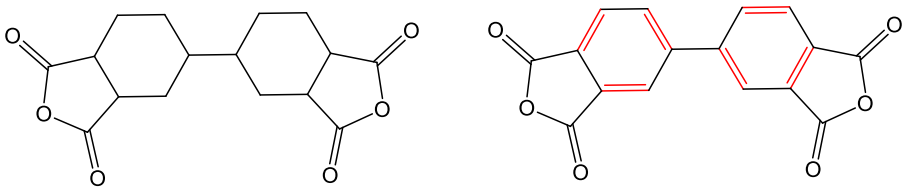

Dicyclohexyl-3,4,3',4'-tetracarboxylic dianhydride (DCDA)

3,3',4,4'-biphenyltetracarboxylic dianhydride (BPDA)

Scheme S1. The molecular structures of the non-aromatic (DCDA) and aromatic (BPDA) dianhydrides.

Table S-I. The Mw, Mn and PDI as calculated from the major peak obtained in GPC. T_g obtained from DSC and rheology.

Polymer	Mw (g/mol)	Mn (g/mol)	PDI	DSC- T_g[a] (°C)	Rheology- T_g[b] (°C)
DCDA-D	21k	12k	1.8	10	22
BPDA-D	37k	20k	1.9	22	33[I], 46[II]

[a] T_g was calculated from the 2nd heating curve, 10°C/min.

[b] T_g was taken as the maximum of the peak in the *tan δ* curve from the rheological temperature sweeps, performed in cooling ramp, 1°C/min (Figure S1 b). These temperatures were used as annealing and healing temperatures (in case of BPDA-D, the temperature of the first peak was used).

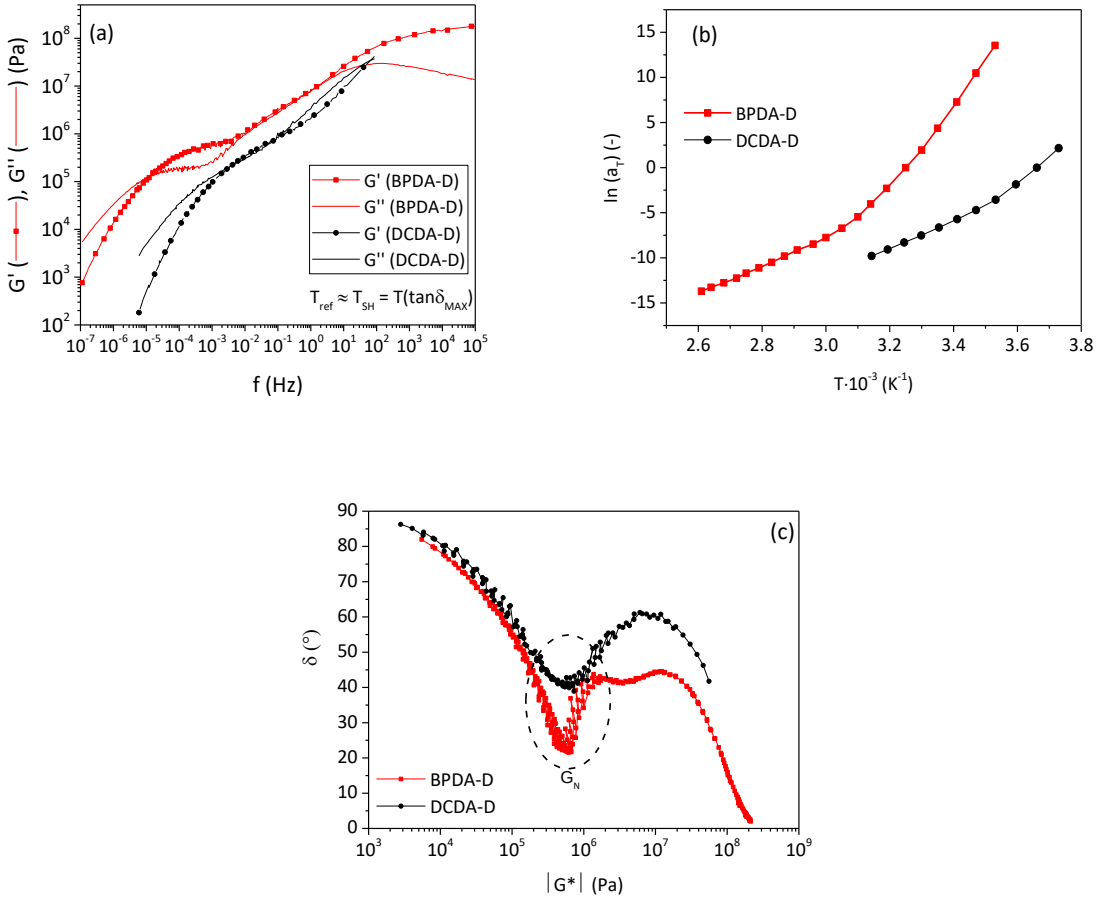

Figure S5. (a) TTS curves of the aromatic BPDA-D and non-aromatic DCDA-D branched polymers; (b) shift factors as function of temperature and aromatics; and (c) van Gurp-Palmen plot used for G_N and M_e calculations.

Table S-II. Characteristic rheological parameters extracted from the TTS mastercurves at $T_{ref} \approx T_{SH} = T_{tan\ \delta\ MAX}$

Polymer	f_s (Hz)	f_d (Hz)	f_g (Hz)	τ_s (s)	τ_d (s)	τ_g (s)	$tan\delta_{MAX}$ (-)	G' slope at $f<f_s$	G'' slope at $f<f_s$	G' slope elastic plateau	G_N* (Pa)	$M_{e,\ app}$** (g/mol)	M_x*** (g/mol)
DCDA-D	$3.5 \cdot 10^{-2}$	0.089	70.0	28.6	11.2	0.01	1.7	1.37	0.83	0.34	$4.8 \cdot 10^{5}$	5420	843
BPDA-D	$1.3 \cdot 10^{-5}$	/	/	$7.7 \cdot 10^{4}$	/	/	0.9	1.27	0.81	0.72	$5.7 \cdot 10^{5}$	4680	831

* G_N calculated from the van Gurp-Palmen plot, $\delta(|G|^*)^2$, (Figure S5, SI)

** $M_{e,\ app}$ (apparent) were calculated according to $M_e = \rho RT/G_N$ (Doi and Edwards) equation, using experimentally determined densities. In this case M_e values must be considered as pseudo-M_e values governed by 'transient interactions', not as molecular weight between entanglements.[2]

*** M_x = average molecular weight between the two neighboring temporal junctions, in this case the DD1 side-chains.

[2] Susa, A.; Bose, R. K.; Grande, A. M.; van der Zwaag, S.; Garcia, S. J., Effect of the dianhydride/branched diamine ratio on the architecture and room temperature healing behavior of polyetherimides. *ACS Applied Materials & Interfaces* **2016**, 8 (49), 34068–34079.

Calculation of rotation energies

To gain further insight on the flexibility of the different dianhydrides as function of their structural differences, a prediction was made using calculated rotation energy profiles of the dianhydrides around the different linkers. The energy of rotation is defined as the maximum energy difference between the different conformers of the dianhydride molecules. All energies and structural optimizations of the isolated molecules in the gas phase were calculated using density functional theory using a RB3LYP 6-31G* basis set. For BPDA, the energy of rotation was simply calculated while gradually changing the dihedral angle between the two phtalic anhydride rings (C1, C2, C3, C4). Because ODPA and 6FDA have two bonds that can be freely rotated, the dihedral angles C1-O2-C3-C4 and C1-C2-C3-C4 were fixed (Figures S6 and S7) after which structure was optimized in energy. The resulting energy of the molecule was recorded and plotted versus the dihedral angle (Figures S5-S8).

According to the results obtained, ODPA showed the lowest energy barrier for rotation, 3.5 kJ/mol, which is caused by the flexible ether (-O-) linker. BPDA and 6FDA showed similar barriers for rotation, 14 kJ/mol and 15 kJ/mol, respectively, although the energy profiles for rotation are different (discussed in the manuscript). In the case of 6FDA, the bulky fluor-containing -CF_3 groups hinder the rotation only close to the highest energy conformer, whereas in BPDA the steric hindrance of the hydrogen atoms on the phtalic anhydride ring causes the maxima in energy to be broader.

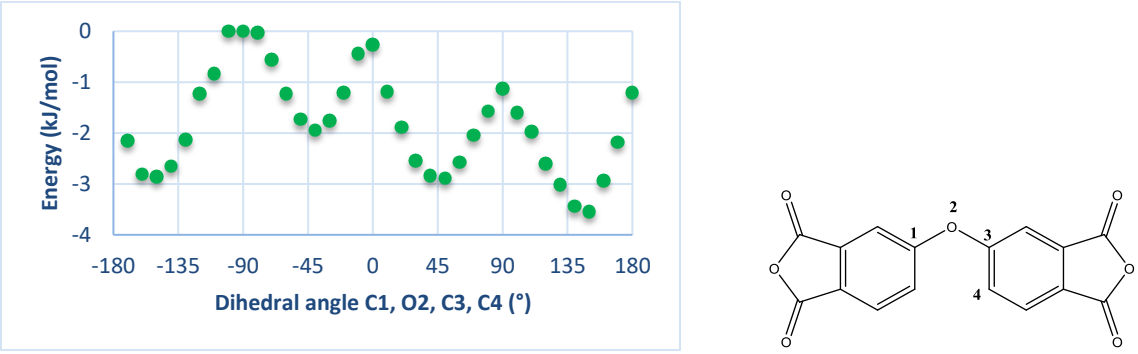

Figure S6. Rotation energy profiles of the ODPA

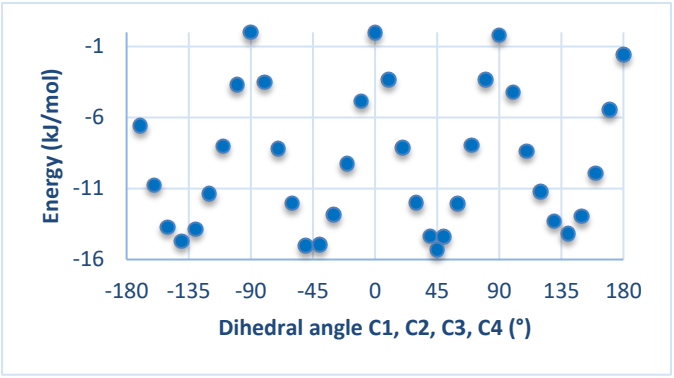

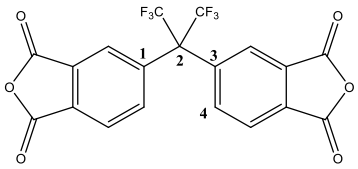

Figure S7. Rotation energy profiles of the 6FDA

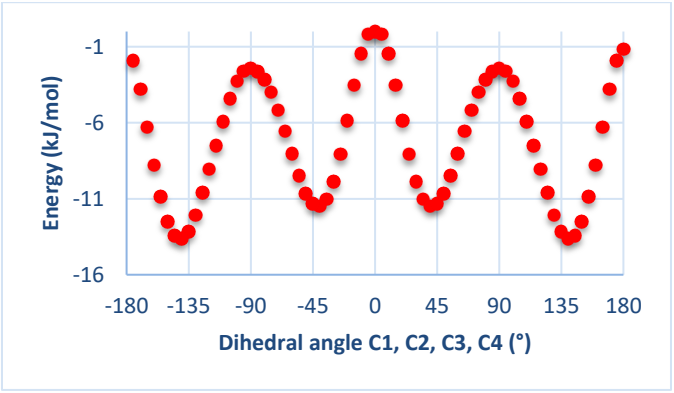

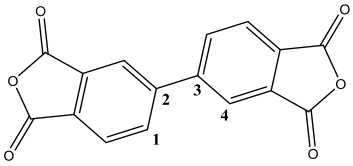

Figure S8. Rotation energy profiles of the BPDA

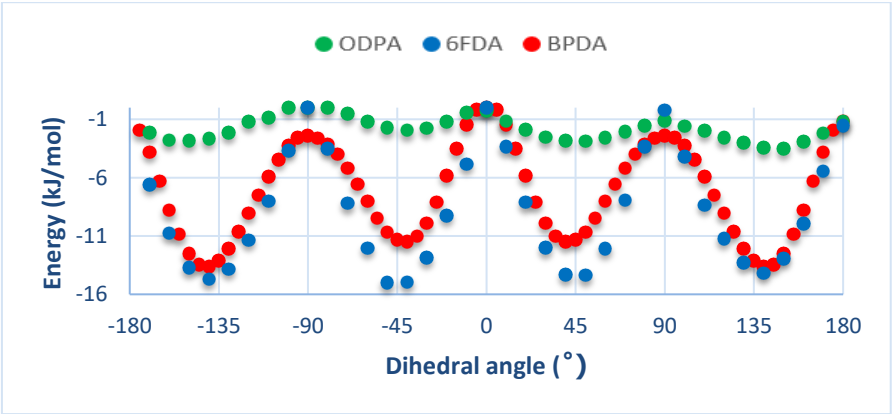

Figure S9. Rotation energy profiles of the three dianhydrides combined in one plot for comparison.